

Modelling Amazon fire regimes under climate change scenarios

Leonardo A. Saravia ^{1 4}, Ben Bond-Lamberty ², Samir Suweis ³

1. Centro Austral de Investigaciones Científicas (CADIC-CONICET), Ushuaia, Argentina.
2. Pacific Northwest National Laboratory, Joint Global Change Research Institute, 5825 University Research Court #3500, College Park, MD 20740, USA
3. Laboratory of Interdisciplinary Physics, Department of Physics and Astronomy “G. Galilei,” University of Padova, Padova, Italy
4. Corresponding author e-mail lsaravia@campus.ungs.edu.ar, ORCID <https://orcid.org/0000-0002-7911-4398>

Abstract

Fire is one of the most important disturbances of the earth-system, shaping the biodiversity of ecosystems and particularly forests. Climatic change and other anthropogenic drivers such as deforestation, land use change, could produce potentially abrupt changes in fire regimes, triggering more profound transformations like the transition from forests to savannah or grasslands ecosystems. Large biodiversity loss could be produced if these transitions occur. Climate change could enhance fire ignition and spread, potentially producing more extensive, intense, and frequent fires. In this work, we use a simple forest-fire model and analyze the possible changes in the Amazon region's fire regime that depend on climate change-related variables. We parameterize this model using remote sensing data on fire extension and temperature, by considering climate projections for the 21st century, and find that there are two possible regime changes: a critical regime that implies high variability in fire extension and mega-fires, and an absorbing phase transition which would produce the extinction of the forest and transition to a different vegetation state. The fitted model and projections suggest that the Amazon region is not close to any of these regime changes and predicts a consistent increment in fire extension. Nonetheless, this increment combined with the factors not considered in the model, such as deforestation, may cause drastic changes in the region.

Introduction

Very few regions in the terrestrial biosphere are unaffected by fire. Fires caused directly or indirectly by human activities (Bowman et al. 2020) have different characteristics from natural fires, including in spatial pattern, severity, burn frequency and seasonality, producing contrasting ecological consequences (Steel et al. 2021). Recent years have seen an increase in fire intensity and extension in different regions (Bowman et al. 2020, Pivello et al. 2021), partially attributable to the fact we are experiencing a biosphere that is 1°C above historical records (Masson-Delmotte et al. 2021); also, it is hypothesized that this intensification could reduce the spatial and temporal variation in fire regimes, called pyrodiversity (Kelly and Brotons 2017), that in turn will generate substantial reductions in biodiversity and ecosystem processes such as carbon storage (Dieleman et al. 2020, Furlaud et al. 2021). It is likely that the most affected regions will be the ones in which fire has been historically rare or absent. In regions such as tropical forests (Barlow et al. 2020), extreme fires could trigger extensive biodiversity loss as well as major ecosystems changes as transitions from forest to savannah or shrublands (Hirota et al. 2011, Fairman et al. 2015).

Fires in the Amazon region were historically rare, due to the ability of old-growth forest to maintain enough moisture to prevent fire spread, even after prolonged drought periods (Uhl and Kauffman 1990). Human activities such as deforestation and land-use change over the past 40 years have produced the conditions for

fire to become much more frequent and widespread across the basin (Alencar et al. 2011, Aragão et al. 2018, Cardil et al. 2020). Droughts are predicted to increase due to climatic change, and have the potential to interact with human activities such as secondary vegetation slash-and-burn and cyclical fire-based pasture cleaning (Aragão et al. 2018). Although deforestation rates were substantially reduced until 2018 (Feng et al. 2021), previous deforestation activities may provide sufficient ignition sources for fire to expand into adjacent forests (Aragão et al. 2018). This process could increase the importance of fires unrelated to deforestation (Aragão et al. 2014).

Different models of fire for the Amazon have been developed to predict regime changes under climate change scenarios. These models can be process-based (Le Page et al. 2017) or statistical (Fonseca et al. 2019), and generally consider land-use change and other human activities, as well as local weather conditions, but they usually neglect the spatial dynamics of fire spread. Statistical fire models take into account mainly environmental factors (Turco et al. 2018), while others simulate more detailed processes (Thonicke et al. 2010), and a few treat spatial dynamical phenomena (Schertzer et al. 2014). Such spatial dynamics are important because they can provide insights into how local interactions give rise to emergent fire patterns (Pueyo et al. 2010), and potentially change the stability characteristics of the entire dynamical system (Levin and Durrett 1996).

Simple models of fire have been used as an example of self-organized criticality (SOC), where systems can self-organize into a state characterized by power-laws in different model outputs. For example, the forest fire model of Drossel & Schwabl Drossel and Schwabl (1992) (DSM) was proposed to show SOC in relation to the size distribution of disturbance events (Jensen 1998). Power-laws imply scale invariance, meaning that there is no characteristic scale in the model. Later it was shown that DSM does not exhibit true scale invariance (Grassberger 2002) and that the system needs to be somewhat tuned to observe criticality (Bonachela and Muñoz 2009). These facts diminished its theoretical attractiveness, but the model could be still of high practical relevance. Some modifications of the Drossel & Schwabl (DSM) model have been used to predict fire responses to climate change (Pueyo 2007), and other DSM variants can reproduce features observed in empirical studies (Ratz 1995) such as the power-law distributions of the fire sizes, the size and shape of unburned areas and the relationship between annual burned area and diversity of ecological stages (Zinck and Grimm 2009). An analysis of different models showed that the key for reproducing all these patterns was changing the scale of grid cells to represent several hectares, and the ‘memory effect’: flammability increases with the time since the last fire at a given site (Zinck and Grimm 2009, Zinck et al. 2011). But the exponent of the fire size distribution observed in different ecoregions still cannot be reproduced by these models.

These simple models could have critical behaviour characterized by power-law distribution in fire sizes and

other model outputs. Such dynamics can be explained in terms of percolation theory (Stauffer and Aharony 1994) where there is a transition between two states: one where propagation of fires occurs, and another where it is very limited. The narrow region where the transition occurs is the critical point, characterized by an order parameter (fire size) that depends on some external control parameter (e.g. ignition probability) (Solé and Bascompte 2006). An example of this transition could be the case of the recent Australia 2019-2020 mega-fires (Nolan et al. 2020). Historically, indigenous fire stewardship in Australian landscapes maintained flammable forest in a disconnected state by producing frequent small scale fires (“Biodiversity in flames” 2020). This regime was disrupted by fire suppression related to European colonization land-use change (Hoffman et al. 2021) and climate (Adams et al. 2020), pushing the system towards a critical regime (Nicoletti et al. 2021). These kinds of extreme events are very difficult to predict by Earth system models that do not fully incorporate the dynamic of fuel accumulation and vegetation dynamics (Sanderson and Fisher 2020).

The objective of this work is to model and predict the changes in fire regimes of the Amazon region using a simple spatial stochastic fire model, based on variables like precipitation and temperature that are included in climate change scenarios. By doing this we are assuming that the emergent dynamics can be described by a process of slow accumulation of fuel and rapid discharge produced by the fires. We first analyse the fire dynamics of the last 20 years in the region with the MODIS burnt area product to check our main assumption and derive an ignition probability. Then we predict the ignition probability up to the year 2060 based on different greenhouse gas Representative Concentration Pathways. Finally, using the model forced with the ignition probability, we predict and analyse the possible changes in the modelled fire regimes for the Amazon.

Methods

Our region of study is the Amazon Basin (Figure S1). This includes Brazil, which represents 60% of the area, as well as eight other countries (Bolivia, Colombia, Ecuador, Guyana, Peru, Suriname, Venezuela, and French Guiana). We chose this region because a significant amount of fires extend to tropical moist forest outside Brazil (Cardil et al. 2020), and the whole area is thought to be a crucial tipping element of the Earth-system (Staver et al. 2011, Lenton and Williams 2013).

Fire data and parameters

We estimated the monthly burned areas from 2001 to the end of 2021 using the NASA Moderate-Resolution Imaging Spectroradiometer (MODIS) burnt area Collection 6 product MCD64A1 (Giglio et al. 2016), which

has a 460 m pixel resolution. We used Google Earth Engine with the JavaScript programming language to download the data restricted to the region of interest (See source code availability below). Each image represents the burned pixels as 1 and the non-burned as 0. We then calculated the burned clusters using 4 nearest neighbours (Von Neumann neighbourhood) and the Hoshen–Kopelman algorithm (Hoshen and Kopelman 1976). Each cluster contains contiguous pixels burned within a month and this represents a fire event S , allowing us to calculate the number and sizes of fire clusters by month. We estimated the probability of ignition f as $f(t) = \frac{|S_t|}{T}$, where $|S_t|$ denotes the number of clusters, S_t that start in the month t (if a fire started in the previous month we avoided it to remove possible double counting), and T is total number of pixels in the region, to allow comparisons with the fire model.

We also estimated the distribution of fire sizes using an annual period to have enough fire clusters to discriminate between different distributions. We aggregated the monthly images using a simple superposition; the annual image has a 1 if it has one or more fires during the year, and 0 if it has none. This assumes that most of the sites only burn once a year, we verified this using the MODIS data that on average only 0.06% burn more than once annually. After that, we ran again the Hoshen–Kopelman algorithm to obtain the annual fire clusters. Then we fitted the following distributions to the fire sizes: power-law, power-law with exponential cut-off, log-normal, and exponential. We used maximum likelihood to decide which distribution fit the data best using the Akaike Information Criteria (AIC) (Clauset et al. 2009). Additionally, we computed a likelihood ratio test, Vuong’s test (Vuong 1989), for non-nested models. We only considered it a true power-law when the value of the AIC was at a minimum and the comparison with the exponential distribution using the Vuong’s test was significant with $p < 0.05$; if $p \geq 0.05$ we assumed that the two distributions cannot be differentiated.

Modelling the probability of ignition

We calculated the monthly ignition probability f and related it to monthly precipitation (ppt), maximum temperature (T_{max}) and a seasonal term (m). These variables have generally been included in global and regional fire activity models (Huang et al. 2015, Turco et al. 2018, Fonseca et al. 2019, Wei et al. 2020). More variables were used in these models, but we are constrained by the variables available in the Climate Projections (see below). We obtained environmental data from the TerraClimate dataset (Abatzoglou et al. 2018), doing an average over the region of study, aiming to represent the influence of regional climate over f . We evaluated an increasingly complex series of generalized additive models (GAMs), assuming a Gaussian distribution and transformed f to logarithms, because it had a highly skewed distribution. Additionally we fitted the same models assuming a Gamma distribution and no transformation for f . For all the models we

used thin plate regression splines (Pedersen et al. 2019) as smoothing terms, and for interactions between environmental variables we used tensor products, using restricted maximum likelihood (REML) to fit to the data (Pedersen et al. 2019). All these procedures were available in the R package `mgcv` (Wood 2017) and all source code is available at the repository <https://github.com/lisaravia/AmazonFireTippingPoints>.

We selected the best models using *AIC* (Wood 2017). To evaluate the predictive power of the models, we broke the data set into a training set representing 85% of the data and testing set (always 3 years long) and we repeated the procedure 10 times starting at different random dates. We then calculated the mean absolute error (MAE) and the Root Mean Squared Error (RMSE) for the three best models selected with *AIC* (Table S2). The formulas of the MAE and RMSE are as follows:

$$\text{MAE} = \frac{1}{n} \sum_{i=1}^n |f_i - \hat{f}_i|$$

$$\text{RMSE} = \sqrt{\frac{1}{n} \sum_{i=1}^n (f_i - \hat{f}_i)^2}$$

Where f_i is the observed ignition probability f at month i , \hat{f}_i the predicted f and n the total number of months used for predictions. We used the model with smaller MAE and RMSE to obtain predictions of the ignition probability up to 2060. Driving data were obtained from the NASA Earth Exchange Global Daily Downscaled Climate Projections NEX-GDPP (<https://www.nccs.nasa.gov/services/data-collections/land-based-products/nex-gddp>)(Thrasher et al. 2012), which were estimated with General Circulation Models (GCM) runs conducted under the Coupled Model Intercomparison Project Phase 5 (Taylor et al. 2012). We averaged over the 21 CMIP5 models and over the study region to obtain the monthly values of the needed variables: precipitation and maximum temperature. Then we estimated the probability of ignition up to 2060 using the fitted GAM across two of the four Representative Concentration Pathways (RCPs), RCP4.5 and RCP8.5 (Meinshausen et al. 2011). Such RCPs are greenhouse gas concentration trajectories adopted by the IPCC and used for climate modelling and research (Moss et al. 2010).

Fire Model

Conceptually the model represents two processes: forest burning and forest recovery. We assume that the forest layer represents the flammable forest (rather than forest cover), and that when a site is burned it does not mean that all the vegetation is dead, but that all the fuel is consumed.

The model uses a 2-dimensional lattice to represent the spatial region. Each site in the lattice can be in one of three different states: an empty or burned site, a flammable forest (called forest for short), or a burning forest. The lattice is updated in parallel, according to the following steps:

1. We pick at random a burning site, and it becomes an empty site in the following step (the model's

timestep is one day)

2. We pick at random a forest site and it becomes a burning forest if one or more of its four nearest neighbour sites are burning
3. We pick at random another forest site and it sends (with probability p) a propagule to an empty site at a distance drawn from a power-law dispersal kernel with exponent d .
4. A random site can catch fire spontaneously with probability f , i.e., this probability changes by month, reflecting the fire season.

We assumed absorbing boundary conditions and a lattice size of 450x450 sites, but also ran simulations with other sizes, resulting in equivalent results. Rule 3 means that a burned or empty site can become forest more quickly when it is near a forest site, but also that some sites can become forest even when far from established forest sites—depending on the kernel exponent, it could be any site in the lattice (Marco et al. 2011). The choice of a power-law dispersal is justified because forests dispersion generally exhibits fat-tailed kernels (Clark et al. 2005, Seri et al. 2012).

This model is very similar to the Drossel-Schwabl forest fire model (Drossel and Schwabl 1992): it exhibits critical behaviour when $\theta = p/f$ tends to ∞ , and thus must satisfy the condition that $f \ll p$, as is generally observed in natural systems. The model involves the separation between three time scales: the fast burning of forest clusters, the slow recovery of forest, and the even slower rate of fire ignitions. Then in the critical regime there is a slow accumulation of forest that forms connected clusters, and eventually as the ignition probability is very low these clusters connect the whole lattice— here is the link with percolation theory (Stauffer and Aharony 1994)— and a single ignition event can produce big fires. After this, the density of the forest becomes very low and the accumulation cycle begins again. This regime is characterized by wide fluctuations in the size of fires and the density of trees, with both following approximately power-law size distributions. If the ignition probability f is too high fires are frequent, forest sites become disconnected and small fires, with a characteristic size, dominate the system.

One of the features not present in the original forest fire model is that forests can have long-distance dispersal, modifying the distribution of forest clusters, the distribution of fire sizes, and the dynamics of the model. When forest dispersal is limited mainly to nearest neighbours, forest recovery produces clusters that tend to coalesce and form uniform clusters with few or no isolated forest sites. When the forest burns, these isolated forest sites are the points from where the forest recovers (assuming no external colonization); when these are not present there is an increased probability that the forest becomes extinct. When dispersal is long-distance there is an important number of isolated forest sites, thus decreasing the probability of forest

extinction. All these processes are particularly important when θ is low and fires are smaller but more frequent. In dynamical terms there is a critical extinction value θ_{ext} , when $\theta < \theta_{ext}$ the forest become extinct, but the critical value depends on the dispersal distance governed by de .

The second feature not present in the original forest fire model is seasonality. In natural systems, there is a period of the year when environmental conditions produce an increase in the fire ignition probability, and during the rest of the year there is a much lower probability of fires. This forces a periodic accumulation of forest and a short period of intense fires which is called the fire season. Thus, the model has a short period of low θ_{min} and a longer period of high θ_{max} . If both the minimum and maximum θ are in the critical region, the model behaviour, in the long run, will be like the critical regime with maximum fire sizes in the fire season. When θ_{max} is in the critical and θ_{min} outside the critical zone, the model's dynamics regime could have more extreme fires (i.e. be more similar to the critical regime) than an equivalent non-seasonal model. If both θ are outside the critical region the dynamics could be close to the critical extinction zone, but in this case, seasonal differences in fire sizes will be less pronounced.

Increasing the length of the fire season as predicted in climate change scenarios (Pausas and Keeley 2021) will produce the model to spend more time at a lower θ decreasing the connectivity of the forest and the size of fires. Moreover, this could increase the possibility of critical extinction if $\theta_{max} - \theta_{min}$ are below θ_{ext} . In this work we are assuming that the forest is flammable forest; the extinction of this state could mean that environmental conditions become wetter and the forest does not burn anymore. If environmental conditions become dryer the extinction of forest probably means a transition to another type of vegetation and then the conditions to apply this model will no longer hold.

We made a set of exploratory simulations, with a range of parameters compatible with what we found for the Amazon region, to characterize the previously described regimes (Table S3). Using a lattice size of 450x450 sites, we ran the simulations for 60 years with an initial forest density of 0.3 (we found that different initial conditions gave similar results), and used the final 40 years to estimate the total annual fire size, the maximum cluster fire size, the distribution of fire sizes, and the total number of fires. To determine the cluster fire sizes and distributions we used the same methods described previously for the MODIS fire data. We ran a factorial combination of dispersal exponent de and θ and 10 repetitions of each parameter set. First, we ran the experiment with θ fixed, keeping the ignition probability f constant, and then repeated the experiment with seasonality: we simulated a fire season of 3 months each year multiplying f by 10. A dispersal exponent $de \gg 1$ (e.g. $de = 102$) is equivalent to a dispersal to the nearest neighbours, while $de = 2.0155$ corresponds to a mean dispersal distance of 66 sites (Table S3), i.e. long range dispersal.

Fire Model Fitting

As we already estimated the f parameter from the 21 years of MODIS data, we only needed to estimate the dispersal exponent de and the probability p of forest growth. This parameter p is expressed as $r = 1/p$, representing the average number of days for forest to recover. For this estimation we duplicated the extension of the estimated f as if it started in 1980; we allowed 20 years for transient effects to dissipate in the model, and then used the last 20 years to compare with monthly fire data. This choice was justified because most human activities in the Amazon started in this decade during the conversion of large areas of forest to agriculture (Brando et al. 2019).

To explore the parameter space we used Latin-hypercube sampling (Fang et al. 2005) with parameter ranges $2.5 - 2.00035$ for de (equivalent to a mean dispersal distance range of 3 - 290 sites) and $365 - 7300$ days for r . As the model has a long transient period, we could suppose that the system is in a transient state thus we also estimated the initial forest density as a parameter with a range of densities of 0.2 - 0.7. We used 600 samples and 10 repeated simulations of the model for each sample, totalling 6000 simulations. We select the best parameter set using Approximate Bayesian Computation (ABC) (Csilléry et al. 2010, 2012) comparing the relative monthly fire size i.e the absolute size divided by the total number of sites (the number of MODIS pixels for the Amazon basin or the number of lattice sites for simulations) with model predictions using euclidean distance. During an initial test, we observed that the peaks in the model were delayed by 2-3 months; the same happens in more realistic process based models (Thonicke et al. 2010), and as we were not interested in predicting the exact seasonal fire patterns, instead of using the complete monthly time series we used the monthly maximum fire size of the year. We validated this choice using a random model simulation with known parameters as data and verifying that we recover the parameters (see source code). The second step of our fitting procedure was to use power-law fire distribution to perform another ABC; to do this we ran 10 simulations for each of the parameter sets in the posterior distribution and then calculated the fire cluster distributions using the same methods explained previously. We use ABC to select a second posterior parameter distribution compared to the median value of the power-law exponent from MODIS data. The tolerance (proportion of results accepted nearest the target values) for both ABC procedures was set at 0.05. Finally, we ran the model with the final posterior parameter distribution, the ignition probability estimated from the MODIS data, and the ignition probability estimated with the GAM model for the period 2000-2020, to check if the data fit with the range of predictions. We performed the ABC using a lattice size of 450×450 sites, and as we used relative values (e.g. absolute fire size divided by the total number of sites) the model does not represent a defined scale.

Model Predictions

We used the posterior parameter distribution set and the predictions of the parameter f under RCP4.5 and RCP8.5 to make simulations up to 2060. We started simulations in the year 1980 as in the fitting procedure, but instead of using f derived directly from data we used the f obtained from the GAM model, allowing us to compare actual and predicted fires using the same method to obtain f .

Results

The monthly fires follow a strong seasonal pattern with a maximum between September and October (Figure S2). We characterize the annual fire regime using the total fire size (total burned area) and the maximum fire cluster (the biggest fire event S_{max}). We note that the years with highest S_{max} are also years with high total fire size (Figure 1). The years 2007 and 2010 had the two highest S_{max} and they also have a power-law distribution (Table S1, Figures S3-S5). Power-law distributions are defined as $cS^{-\alpha}$ where c is constant, α the exponent and have an extra parameters: $S = x_{min}$, which is the minimum value for which the power-law holds. The constant c is given by the normalization requirement (Newman 2005). Only 6 of 20 years exhibit fire sizes following a power law distribution (Table S1), and some of such distributions have a range $[S_{max} - x_{min}]$ with the highest values compared to the years without power-laws, but there are also years with power-law and small range. These two extremes represent a pattern that we also observe in the fire model.

We fitted GAM models for the ignition probability f with single variables, combinations of two interacting variables, and one month lags, the best model with lower AIC and lower MAE and RMSE was the Gaussian with the interaction $T_{max} * m$ (Table S2). For the GAM fitted to the complete dataset we observe that the model does not capture the most extreme years of f (Figure S7), but the model fitted for the first years (< 2018) predicted the rest of the data well (Figure S8).

With the best-fitted GAM and the T_{max} from the NASA Earth Exchange Global Daily Downscaled Climate Projections, we predicted the monthly f starting from 2021 for two greenhouse gas emissions scenarios: RCP4.5 and RCP8.5. For the fire model simulations we added the GAM's predictions using the actual data previous to 2021, we can observe that the temporal pattern of f before 2021 are seasonal but more irregular and variable than the patterns after 2021 (Figures S9 & S10).

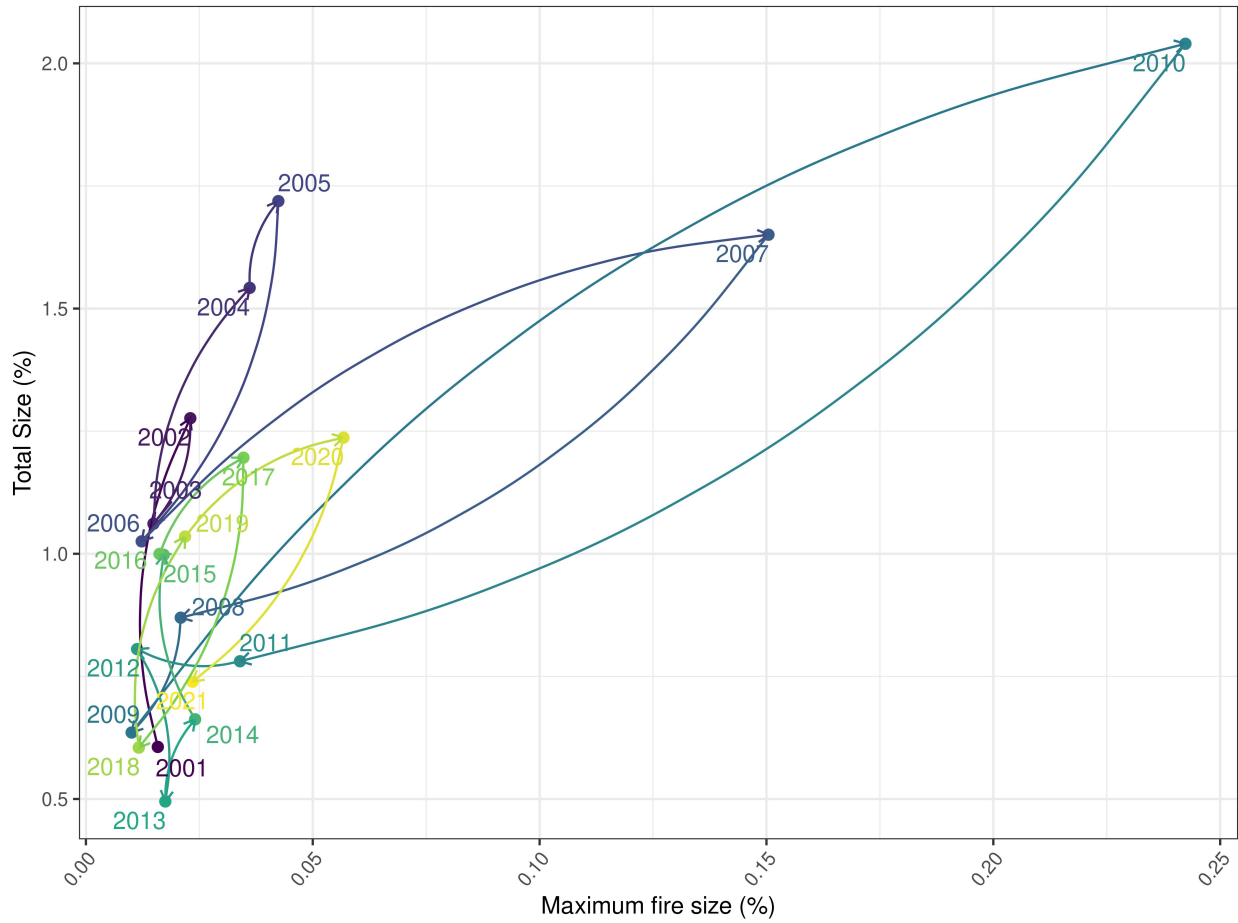


Figure 1: Annual total fire size vs maximum fire size relative to Amazon basin, estimated with MODIS burned area product. These observed data exhibit cycles of loading and discharge, years with high fire extension and big fire events—the upper right region of the figure—which are followed by years of low fire extension and no extreme events in the lower left region. A typical trajectory could be the years 2009, 2010 and 2011 where this cycle can be clearly observed.

Fire model exploration

We ran the model for a range of the $\theta = p/f$ parameter, anticipating that larger values would produce critical behaviour, consisting of large variability of fires between years and extremely large cluster fire sizes that follow a power-law distribution. As expected, we obtained a larger proportion of power-law distributions for the biggest size of θ (Table S4 & S5), and particularly high variability and extremely big fires (Figure 2). For simulations with seasonality, we observed the expected decrease on the number of years where fire cluster size follow power law distribution, also less variability and fewer extreme fires, because in these cases θ decreases for the fire season. Seasonality also had the unexpected effect of increasing the frequency of power-law distribution for $\theta = 25$ with a bigger exponent than the ones for large θ (Table S5); this pattern was also observed in the MODIS data.

In the simulations with $\theta = 25$ and 250 and with shorter dispersal distances, the forest density tends to decrease and eventually, it reaches zero, marking the absorbing phase transition reported for this type of model (Nicoletti et al. 2021), meaning that in these cases the parameter θ was below the critical point θ_{ext} (Figure S11). Increasing the dispersal distance produces higher forest density, while seasonality has the opposite effect. In the case of high dispersal and low θ and seasonality, we are again below θ_{ext} . Note that forest density is the so-called active component of the model and represents the flammable forest.

Fire Model Fitting

After the first ABC we obtained the first posterior distribution of parameters (Table S6). The model generated simulations that closely resemble the monthly MODIS fire estimates, despite being fit only using annual maxima (Figure S14). Repeated simulations with the same set of parameters revealed significant variation due to the stochastic nature of the model dynamics (Figure S14 & S15). A noticeable lag in the model's monthly maxima compared to MODIS data (Figures S14 & S15) may be due to the lack of a fire spread velocity parameter in the model. Despite this, when evaluating the total annual fire size, the model produced intervals that encompassed the MODIS estimates (Figure S16). Thus, the lag in the monthly maxima does not significantly impact our goal of predicting the total annual fire.

For the second ABC we used the posterior obtained in the first step, and calculated the power law exponent of the model simulations; this new set of parameters had a similar range as the first (Table S7), with simulated power law exponents near the observed value (Figure S17). The average θ of the final posterior distribution have a mean of 61 a range between 9 and 910, which is a low-intermediate range, considering the parameter range we used for the model exploration.

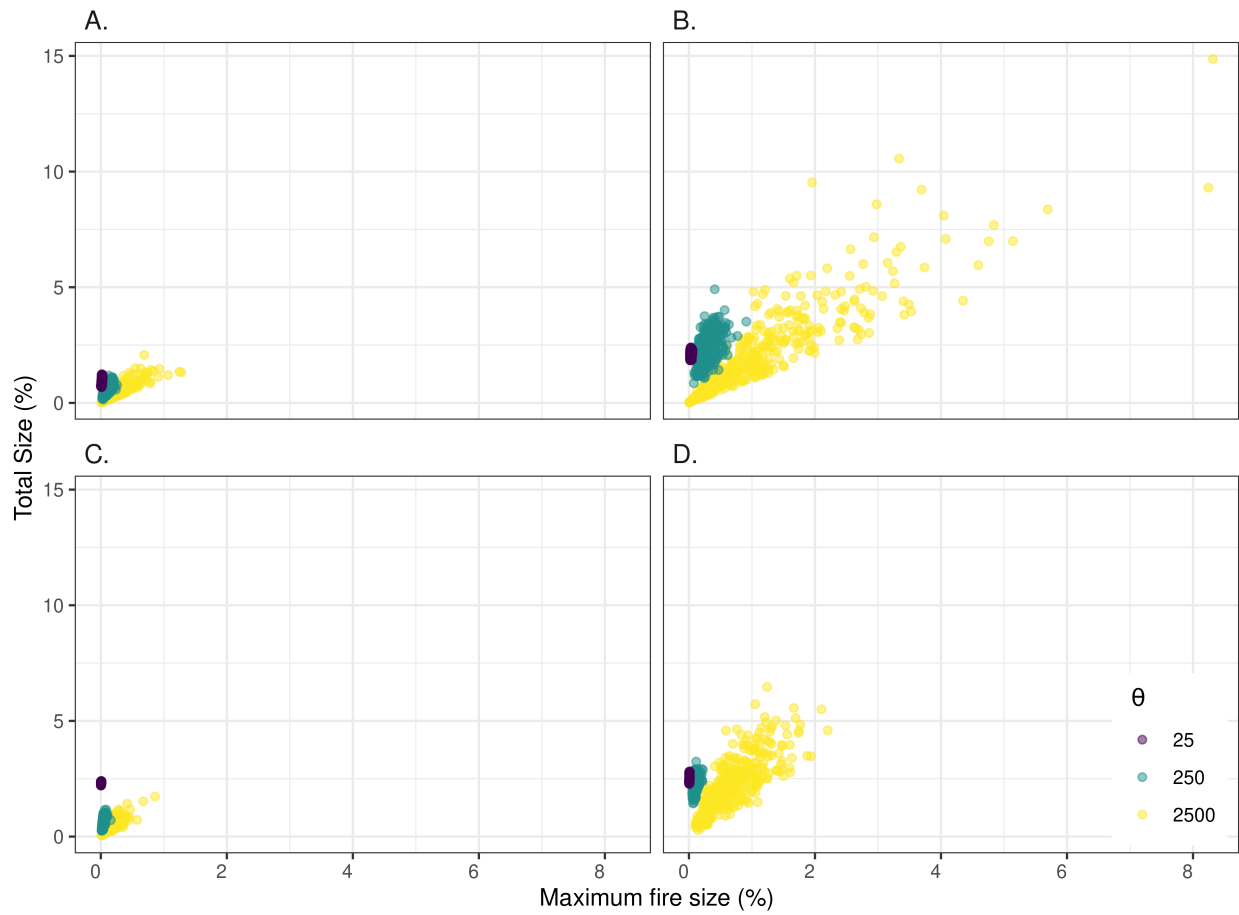


Figure 2: Total annual fire size vs. max fire cluster for the Fire model. **A** & **B** Are simulations with fixed θ , **A** with dispersal exponent $de = 102$, mean dispersal distance of 1 (equivalent to nearest neighbours) and **B** with $de = 2.0155$, mean dispersal distance of 66 sites. **C** & **D** Are simulations with a fire season of 90 days where θ is divided by 10 (the probability of ignition f is multiplied by 10), and the same de as previously.

When observing the predictions without temporal structure (Figure 3), the model simulated with the ignition probability f calculated from the data, and f estimated using the GAM model, gave results consistent with the observed data range. The predicted total fire size has a very good match with the data, while the predicted number of fires is slightly higher; S_{max} is moderately higher and the power-law exponent α of the fire size distribution is lower (Figure 3); these results are inter-related because when α is lower we expect larger fire events (Figure 3).

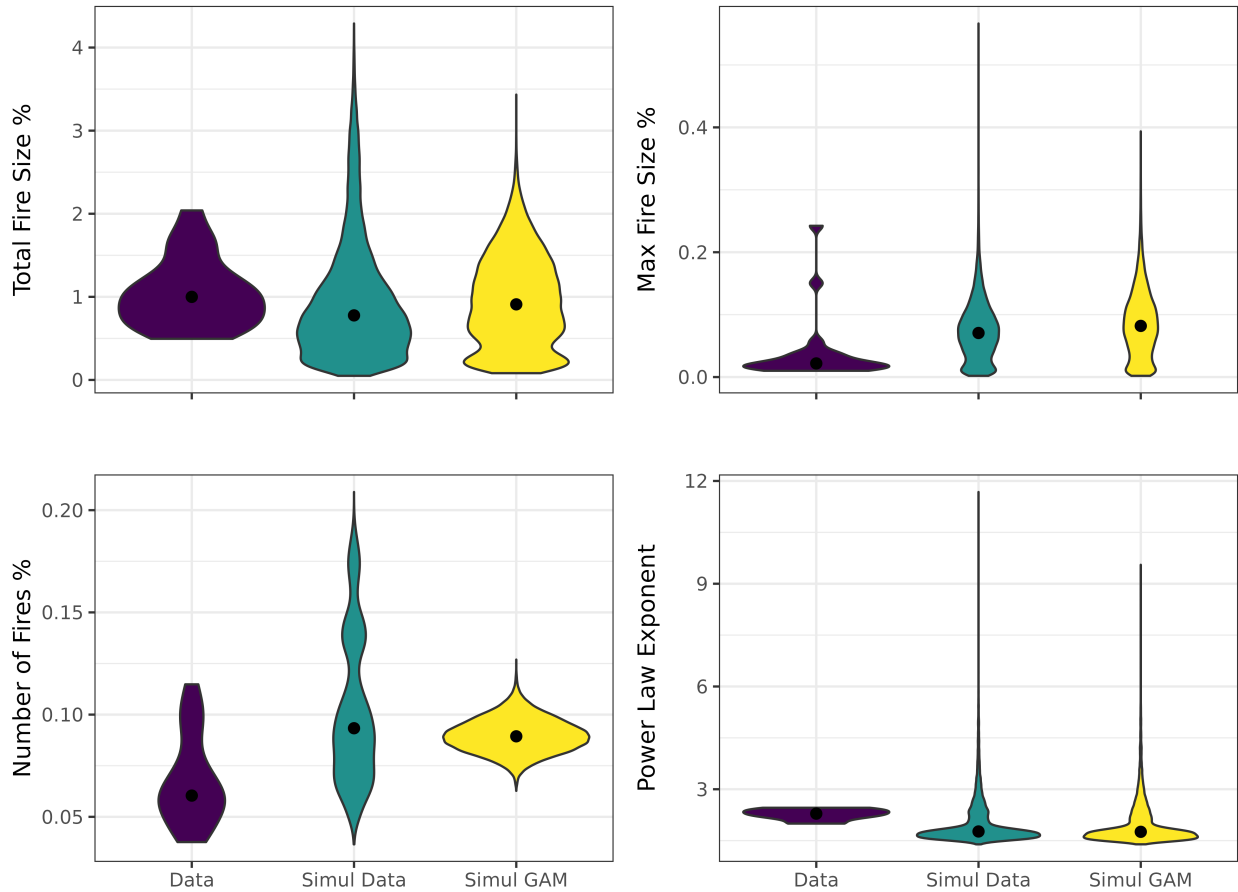


Figure 3: Predictions of the fire model compared with observed data for the years 2001-2020. We used best-fit parameters, the ignition probability from MODIS, and the ignition probability from the estimated GAM models (Simul GAM), and run 100 simulations of the model. To make them comparable we divided all the outputs (except power law exponent) by the total number of pixels in the region/model; black points are the medians.

Fire model predictions

The modelled temporal series, based on the f from the GAM model for the 2001-2021 period, shows a wide 95th percentile interval that encompasses almost all the fire data (with the exception of the 2010 extreme fire). The median of the series suggests a decreasing trend in annual fires over this time period (Figure 4).

After 2021, the model utilizes General Circulation Model (GCM) predictions to estimate the fire ignition f . Under both RCP scenarios, a similar trend of increasing total annual fires is observed, but the annual maxima remain lower than the values observed in the 2001-2021 period.

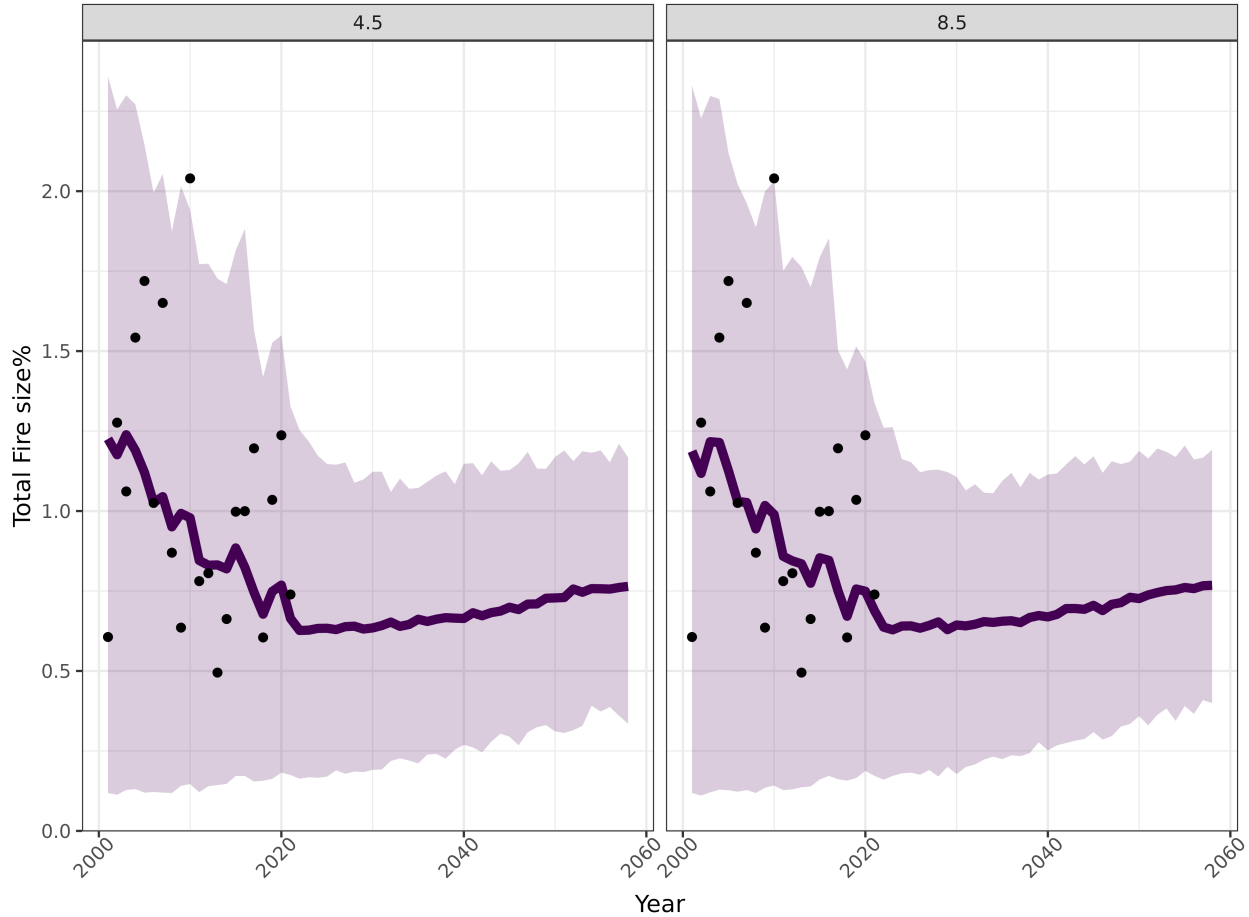


Figure 4: Time series of predictions of the fire model compared with observed data for the years 2001-2060. We used best-fit parameters distribution, the ignition probability from the estimated GAM models based on actual data up to 2021 and based on RCP 4.5, 8.5 afterwards. The points are the actual data, the line the median of simulations with 95% confidence interval bands. All the outputs are relative to the total area.

The trends in the total annual vs maxima by decade fire plot (Figure 5) were consistent with the observations described above. The plot shows all the model simulations, demonstrating that the model is capable of simulating extreme fires, but the expected trend due to climate change scenarios is a decrease in extreme fires and an increase in median annual fire values.

Discussion

Based on spatial forest-fire dynamics, the model fitted to actual data and the predictions up to 2060 suggest that the Amazon fire dynamics are outside an extreme critical regime and far from an absorbing phase

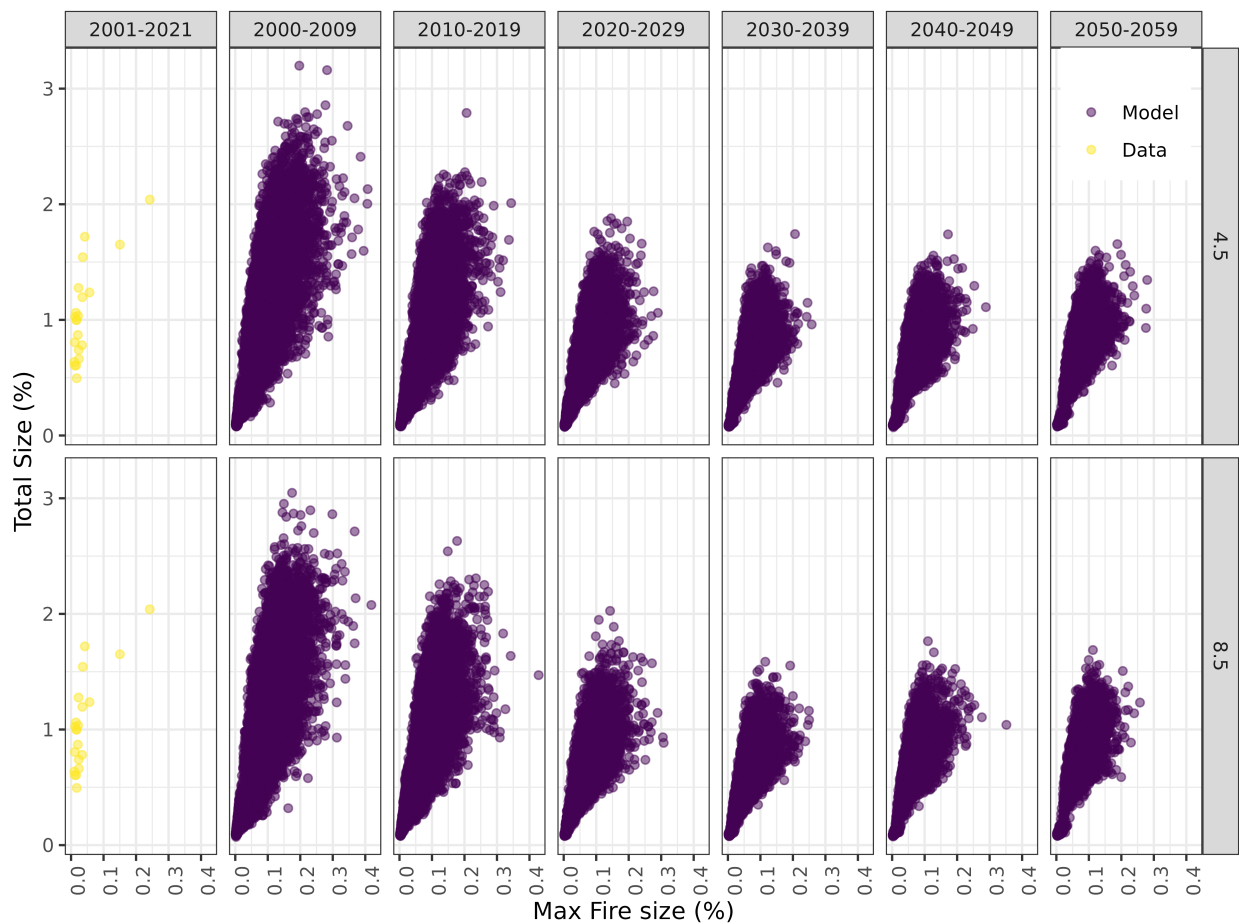


Figure 5: Total annual size of fires vs maximum monthly fire size % relative to the area of the region. The data column was estimated using the MODIS burned area product. The predictions by decade were estimated with a fitted model using a monthly ignition probability calculated with data from General Circulation Models under two greenhouse gas emissions scenarios known as Representative Concentration Pathways (RCPs), RCP4.5 and RCP8.5. For the years 2001-2020 the ignition probability was estimated from actual data.

transition. In addition, the model predicts a reduction of extreme annual fires that might be due to the double average that we used for the General Circulation Models (GCM): we averaged the temperature over the spatial extension of the region and over all the 21 GCM. When we used the actual data —also averaged over the region— the model predicts in the range of observed extreme fires. So we hypothesize that increased temporal variability of the ignition probability could produce an increase in the extreme fires not captured by the model due to the smoothed nature of the CGM data. The increase in median tendency of the annual fires seems a more robust prediction, however, and is in line with the predicted increase in fire weather conditions for the area (Abatzoglou et al. 2019).

A critical regime would imply far more extreme fires and an absorbing phase transition could signal an imminent forest-savanna transition, without extreme fires but with more frequent fires. The actual and predicted fire regime seems to lie between these regimes. This model does not explicitly include deforestation or slash and burn and other agricultural areas—these are implicitly represented in the flammable forest state—and thus the continuous increase of these land uses could combine with the increase in fires and produce drastic changes in the Amazonian region. In its present form, the model predictions represent the influence of climate change through temperature on fire dynamics.

Similar models have been used to fit fire data and determine if the system is in a critical regime. For example, Zinck et al. (Zinck et al. 2011) found that some regions of Canada have experienced a change in the fire regime from a non-critical to critical. They argued that the original Drossel-Schwabl model (DSM) did not give the correct values of the power-law exponent of fire distributions, and thus modified the model to represent fire propagation as a stochastic birth-death process. This means modelling fire as a contact process (Oborny et al. 2007) that develops over the forest sites; the same concept was further explored concerning the recent Australian mega-fires (Nicoletti et al. 2021). Here we took a different approach: as in the DSM in our model fire spread is deterministic, and we added what we think are the minimal processes needed for more realism: seasonality and forest dispersal distance. We agree with Zinck et al. (Zinck et al. 2011) that an extension of the original DSM was needed to represent the fire process observed in ecosystems, but also that not all complexity can or should be added; it is necessary to keep the model tractable in order to e.g. perform parameter-space exploration. Similar models including a deforested state with different ignition f and recovery p probabilities should be built and a rigorous comparison between these types of fire models would be needed to determine which mechanisms are most important to represent.

Our model is phenomenological, in the sense that it does not include all mechanisms present at local scales but tries to predict fire dynamics at broad scales. One of the advantages of this kind of model is that it can be applied to different systems. This is the case of the original DSM model which has been applied to

brain activity and rainfalls (Palmieri and Jensen 2020). In these two systems there are cycles of loading and discharge, a broad region where the fluctuations peak as the critical behaviour is established, and not a critical point with a very sharp transition as the theory of second order phase transitions suggests (Stauffer and Aharony 1994). The temporal dependence of the parameters imposed by the fire seasons, where during some months there is a higher ignition probability f , changes the control parameters with respect to the DMS model since, in fact, we do not observe a transition for a specific value of the θ parameter. Our results suggest that instead of having a specific fine-tuning to observe critical fire spread, a critical region similar to a Griffiths phase (Moretti and Muñoz 2013) may be present in our model. However, we lack a rigorous result in this regard.

We observed the expected effect of the drought in 2010 on fires: the Amazon basin experienced the most extensive fires of the record, despite the deforestation rates being substantially lower than in the previous decade (Aragão et al. 2018). Other years of drought did not have the same effect, and the drought associated with the El Niño event in 2015-2016 produced a considerably lower number of fires than the 2010 drought. This difference could be explained by the nonlinear loading and discharge cycles that characterize the dynamics of fire-forest systems: after the fires and drought the fuel build up during the wetter years so the effects of an extreme could be different. It has been observed that deforestation as a cause of fires is becoming secondary, with droughts becoming primary producers of fires in the Amazon (Aragão et al. 2018). The good fit of our model, forced with the ignition probability estimated from actual data, supports that hypothesis. Our model incorporates the influence of drought using actual and predicted temperature to model the probability of ignition f . Using the inverse of the p parameter the model also predicts that the forest will be recovered between 13 and 19 years, close to the 23 years suggested by Alencar (Alencar et al. 2011).

The forest state in the model represents the flammable forest, as undisturbed tropical forest in the Amazon is thought to be not flammable and with a very low probability of natural fires (Fonseca et al. 2019). This is changing, however, due to the increased edges of undisturbed forest with human degraded forest and other land uses (Aragão et al. 2018). Fire is still produced by human activities (Barlow et al. 2020) and starts from the transportation network and from the outside regions (Brando et al. 2019). These human-induced fires can invade standing forest and if climate change makes forests hotter and drier it will become more capable of sustaining more extensive fires (Brando et al. 2019). These changes are not considered in our model, and they would imply a higher density of our flammable forest state that could be represented by a lower θ than the estimated one, increasing the likelihood of an absorbing phase transition in which the forest has lost its capacity to recover from frequent fires and droughts (Brando et al. 2019)

Several studies have suggested that a deforestation of 20% to 40% of the Amazon could lead to a rapid transformation into non-forest ecosystems (Nobre et al. 2016, Lovejoy and Nobre 2018). Currently, approximately 20% of the Amazon's forest has been lost since the 1960s and environmental signals suggest that the system is undergoing fluctuations (Lovejoy and Nobre 2018). Dynamic analysis suggests that it is close to a transition point (Saravia et al. 2018). However, our model predicts that the fire regime will not experience a significant change solely due to climate change. Our main conclusion is that if deforestation and degradation of the Amazon forest decrease, the region is likely to be resilient to predicted climate change, and the collapse of the Amazonian tropical forest into a savanna will not occur.

Acknowledgements

LAS is grateful to the Universidad Nacional de General Sarmiento for financial support (Project 30/1139), to the Agencia Nacional de Promoción Científica y Tecnológica (PICT 2020-SERIEA-02628) and Santiago R. Doyle for getting the computational resources used in this work.

Authors' contributions

LAS, BBL, and SS conceived the ideas and designed methodology; LAS collected the data; LAS wrote the code; LAS, BBL and SS analysed the data; LAS led the writing of the manuscript. All authors contributed critically to the drafts and gave final approval for publication.

Data Availability Statement

The source code and data are available at zenodo <https://doi.org/10.5281/zenodo.5703638> and Github <https://github.com/lсарavia/AmazonFireTippingPoints>. Remote sensing MODIS data and climate data are available directly from NASA and Google Earth Engine.

References

- Abatzoglou, J. T. et al. 2018. TerraClimate, a high-resolution global dataset of monthly climate and climatic water balance from 1958. - *Scientific Data* 5: 170191.
- Abatzoglou, J. T. et al. 2019. Global Emergence of Anthropogenic Climate Change in Fire Weather Indices. - *Geophysical Research Letters* 46: 326–336.
- Adams, M. A. et al. 2020. Causes and consequences of Eastern Australia's 2019 season of mega-fires: A broader perspective. - *Global Change Biology* 26: 3756–3758.

- Alencar, A. et al. 2011. Temporal variability of forest fires in eastern Amazonia. - *Ecological Applications* 21: 2397–2412.
- Aragão, L. E. O. C. et al. 2014. Environmental change and the carbon balance of Amazonian forests. - *Biological Reviews* 89: 913–931.
- Aragão, L. E. O. C. et al. 2018. 21st Century drought-related fires counteract the decline of Amazon deforestation carbon emissions. - *Nature Communications* 9: 536.
- Barlow, J. et al. 2020. Clarifying Amazonia’s burning crisis. - *Global Change Biology* 26: 319–321.
2020. Biodiversity in flames. - *Nature Ecology & Evolution* 4: 171–171.
- Bonachela, J. A. and Muñoz, M. A. 2009. Self-organization without conservation: True or just apparent scale-invariance? - *Journal of Statistical Mechanics: Theory and Experiment* 2009: P09009.
- Bowman, D. M. J. S. et al. 2020. Vegetation fires in the Anthropocene. - *Nature Reviews Earth & Environment*: 1–16.
- Brando, P. M. et al. 2019. Droughts, Wildfires, and Forest Carbon Cycling: A Pantropical Synthesis. - *Annual Review of Earth and Planetary Sciences* 47: 555–581.
- Cardil, A. et al. 2020. Recent deforestation drove the spike in Amazonian fires. - *Environmental Research Letters* 15: 121003.
- Clark, C. J. et al. 2005. Comparative seed shadows of bird-, monkey-, and wind-dispersed trees. - *Ecology* 86: 2684–2694.
- Clauset, A. et al. 2009. Power-Law Distributions in Empirical Data. - *SIAM Review* 51: 661–703.
- Csilléry, K. et al. 2010. Approximate Bayesian Computation (ABC) in practice. - *Trends in Ecology & Evolution* 25: 410–418.
- Csilléry, K. et al. 2012. Abc: An R package for approximate Bayesian computation (ABC). - *Methods in Ecology and Evolution* 3: 475–479.
- Dieleman, C. M. et al. 2020. Wildfire combustion and carbon stocks in the southern Canadian boreal forest: Implications for a warming world. - *Global Change Biology* 26: 6062–6079.
- Drossel, B. and Schwabl, F. 1992. Self-organized critical forest-fire model. - *Physical Review Letters* 69: 1629–1632.

- Fairman, T. A. et al. 2015. Too much, too soon? A review of the effects of increasing wildfire frequency on tree mortality and regeneration in temperate eucalypt forests. - *International Journal of Wildland Fire* 25: 831–848.
- Fang, K.-T. et al. 2005. *Design and Modeling for Computer Experiments*.
- Feng, X. et al. 2021. How deregulation, drought and increasing fire impact Amazonian biodiversity. - *Nature* 597: 516–521.
- Fonseca, M. G. et al. 2019. Effects of climate and land-use change scenarios on fire probability during the 21st century in the Brazilian Amazon. - *Global Change Biology* 25: 2931–2946.
- Furlaud, J. M. et al. 2021. Bioclimatic drivers of fire severity across the Australian geographical range of giant Eucalyptus forests. - *Journal of Ecology* 109: 2514–2536.
- Giglio, L. et al. 2016. The collection 6 MODIS active fire detection algorithm and fire products. - *Remote Sensing of Environment* 178: 31–41.
- Grassberger, P. 2002. Critical behaviour of the Drossel-Schwabl forest fire model. - *New Journal of Physics* 4: 17.
- Hirota, M. et al. 2011. Global Resilience of Tropical Forest and Savanna to Critical Transitions. - *Science* 334: 232–235.
- Hoffman, K. M. et al. 2021. Conservation of Earth’s biodiversity is embedded in Indigenous fire stewardship. - *Proceedings of the National Academy of Sciences* in press.
- Hoshen, J. and Kopelman, R. 1976. Percolation and cluster distribution. I. Cluster multiple labeling technique and critical concentration algorithm. - *Physical Review B* 14: 3438–3445.
- Huang, Y. et al. 2015. Sensitivity of global wildfire occurrences to various factors in the context of global change. - *Atmospheric Environment* 121: 86–92.
- Jensen, H. J. 1998. *Self-Organized Criticality: Emergent Complex Behavior in Physical and Biological Systems*. - Cambridge University Press.
- Kelly, L. T. and Brotons, L. 2017. Using fire to promote biodiversity. - *Science* 355: 1264–1265.
- Le Page, Y. et al. 2017. Synergy between land use and climate change increases future fire risk in Amazon forests. - *Earth System Dynamics* 8: 1237–1246.

- Lenton, T. M. and Williams, H. T. P. 2013. On the origin of planetary-scale tipping points. - *Trends in Ecology & Evolution* 28: 380–382.
- Levin, S. A. and Durrett, R. 1996. From individuals to epidemics. - *Philosophical Transactions of the Royal Society of London. Series B* 351: 1615–1621.
- Lovejoy, T. E. and Nobre, C. 2018. Amazon Tipping Point. - *Science Advances* 4: eaat2340.
- Marco, D. E. et al. 2011. Comparing short and long-distance dispersal: Modelling and field case studies. - *Ecography* 34: 671–682.
2021. Summary for policymakers. - In: Masson-Delmotte, V. et al. (eds), *Climate Change 2021: The Physical Science Basis. Contribution of Working Group I to the Sixth Assessment Report of the Intergovernmental Panel on Climate Change*. Cambridge University Press, in press.
- Meinshausen, M. et al. 2011. The RCP greenhouse gas concentrations and their extensions from 1765 to 2300. - *Climatic Change* 109: 213–241.
- Moretti, P. and Muñoz, M. A. 2013. Griffiths phases and the stretching of criticality in brain networks. - *Nature Communications* 4: 2521.
- Moss, R. H. et al. 2010. The next generation of scenarios for climate change research and assessment. - *Nature* 463: 747–756.
- Newman, M. E. J. 2005. Power laws, Pareto distributions and Zipf's law. - *Contemporary Physics* 46: 323–351.
- Nicoletti, G. et al. 2021. The emergence of scale-free fires in Australia. - arXiv:2110.10014 [cond-mat] in press.
- Nobre, C. A. et al. 2016. Land-use and climate change risks in the Amazon and the need of a novel sustainable development paradigm. - *Proceedings of the National Academy of Sciences* 113: 10759–10768.
- Nolan, R. H. et al. 2020. Causes and consequences of eastern Australia's 2019 season of mega-fires. - *Global Change Biology* 26: 1039–1041.
- Oborny, B. et al. 2007. Survival of species in patchy landscapes: Percolation in space and time. - In: *Scaling Biodiversity*. Cambridge University Press, pp. 409–440.
- Palmieri, L. and Jensen, H. J. 2020. The Forest Fire Model: The Subtleties of Criticality and Scale Invariance. - *Frontiers in Physics* 8: 257.

- Pausas, J. G. and Keeley, J. E. 2021. Wildfires and global change. - *Frontiers in Ecology and the Environment* 19: 387–395.
- Pedersen, E. J. et al. 2019. Hierarchical generalized additive models in ecology: An introduction with mgcv. - *PeerJ* 7: e6876.
- Pivello, V. R. et al. 2021. Understanding Brazil's catastrophic fires: Causes, consequences and policy needed to prevent future tragedies. - *Perspectives in Ecology and Conservation* in press.
- Pueyo, S. 2007. Self-Organised Criticality and the Response of Wildland Fires to Climate Change. - *Climatic Change* 82: 131–161.
- Pueyo, S. et al. 2010. Testing for criticality in ecosystem dynamics: The case of Amazonian rainforest and savanna fire. - *Ecology Letters* 13: 793–802.
- Ratz, A. 1995. Long-Term Spatial Patterns Created by Fire: A Model Oriented Towards Boreal Forests. - *International Journal of Wildland Fire* 5: 25–34.
- Sanderson, B. M. and Fisher, R. A. 2020. A fiery wake-up call for climate science. - *Nature Climate Change* 10: 175–177.
- Saravia, L. A. et al. 2018. Power laws and critical fragmentation in global forests. - *Scientific Reports* 8: 17766.
- Schertzer, E. et al. 2014. Implications of the spatial dynamics of fire spread for the bistability of savanna and forest. - *Journal of Mathematical Biology* 70: 329–341.
- Seri, E. et al. 2012. Neutral Dynamics and Cluster Statistics in a Tropical Forest. - *The American Naturalist* 180: E161–E173.
- Solé, R. V. and Bascompte, J. 2006. *Self-organization in Complex Ecosystems*. - Princeton University Press.
- Stauffer, D. and Aharony, A. 1994. *Introduction To Percolation Theory*. - Taylor & Francis.
- Staver, A. C. et al. 2011. The Global Extent and Determinants of Savanna and Forest as Alternative Biome States. - *Science* 334: 230–232.
- Steel, Z. L. et al. 2021. Quantifying pyrodiversity and its drivers. - *Proceedings of the Royal Society B: Biological Sciences* 288: 20203202.
- Taylor, K. E. et al. 2012. An Overview of CMIP5 and the Experiment Design. - *Bulletin of the American Meteorological Society* 93: 485–498.

- Thonicke, K. et al. 2010. The influence of vegetation, fire spread and fire behaviour on biomass burning and trace gas emissions: Results from a process-based model. - *Biogeosciences* 7: 1991–2011.
- Thrasher, B. et al. 2012. Technical Note: Bias correcting climate model simulated daily temperature extremes with quantile mapping. - *Hydrology and Earth System Sciences* 16: 3309–3314.
- Turco, M. et al. 2018. Skilful forecasting of global fire activity using seasonal climate predictions. - *Nature Communications* 9: 2718.
- Uhl, C. and Kauffman, J. B. 1990. Deforestation, Fire Susceptibility, and Potential Tree Responses to Fire in the Eastern Amazon. - *Ecology* 71: 437–449.
- Vuong, Q. H. 1989. Likelihood Ratio Tests for Model Selection and Non-Nested Hypotheses. - *Econometrica* 57: 307–333.
- Wei, F. et al. 2020. Nonlinear dynamics of fires in Africa over recent decades controlled by precipitation. - *Global Change Biology* 26: 4495–4505.
- Wood, S. N. 2017. *Generalized Additive Models: An Introduction with R*, Second Edition. - CRC Press.
- Zinck, R. D. and Grimm, V. 2009. Unifying wildfire models from ecology and statistical physics. - *The American naturalist* 174: E170–85.
- Zinck, R. D. et al. 2011. Understanding Shifts in Wildfire Regimes as Emergent Threshold Phenomena. - *The American Naturalist* 178: E149–E161.